Published in final edited form as:
Mol Microbiol. 2012 August ; 85(4): 782–794. doi:10.1111/j.1365-2958.2012.08139.x.

Two CheW coupling proteins are essential in a chemosensory pathway of *Borrelia burgdorferi*

Kai Zhang[1], **Jun Liu**[3], **Youbin Tu**[4], **Hongbin Xu**[1], **Nyles W. Charon**[5], and **Chunhao Li**[1,2,*]

[1]Department of Oral Biology, State University of New York at Buffalo, New York 14214

[2]Department of Microbiology and Immunology, State University of New York at Buffalo, New York 14214

[3]Department of Pathology and Laboratory Medicine, University of Texas Medical School at Houston, Texas 77030

[4]Department of Bioinformatics, Soochow University, Suzhou 215123, China

[5]Department of Microbiology, Immunology and Cell Biology, Health Sciences Center, West Virginia University, Morgantown, WV 26506

SUMMARY

In the model organism *Escherichia coli*, the coupling protein CheW, which bridges the chemoreceptors and histidine kinase CheA, is essential for chemotaxis. Unlike the situation in *E. coli*, *Borrelia burgdorferi*, the causative agent of Lyme disease, has three *cheW* homologues (*cheW*$_1$, *cheW*$_2$, and *cheW*$_3$). Here, a comprehensive approach is utilized to investigate the roles of the three *cheWs* in chemotaxis of *B. burgdorferi*. First, genetic studies indicated that both the *cheW*$_1$ and *cheW*$_3$ genes are essential for chemotaxis, as the mutants had altered swimming behaviors and were non-chemotactic. Second, immunofluorescence and cryo-electron tomography studies suggested that both CheW$_1$ and CheW$_3$ are involved in the assembly of chemoreceptor arrays at the cell poles. In contrast to *cheW*$_1$ and *cheW*$_3$, *cheW*$_2$ is dispensable for chemotaxis and assembly of the chemoreceptor arrays. Finally, immunoprecipitation studies demonstrated that the three CheWs interact with different CheAs: CheW$_1$ and CheW$_3$ interact with CheA$_2$ whereas CheW$_2$ binds to CheA$_1$. Collectively, our results indicate that CheW$_1$ and CheW$_3$ are incorporated into one chemosensory pathway that is essential for *B. burgdorferi* chemotaxis. Although many bacteria have more than one homologue of CheW, to our knowledge, this report provides the first experimental evidence that two CheW proteins co-exist in one chemosensory pathway and that both are essential for chemotaxis.

Keywords

Lyme disease; *Borrelia burgdorferi*; Chemotaxis; Receptor-kinase coupling protein CheW

INTRODUCTION

Chemotaxis allows motile bacteria to swim towards a favorable environment or away from one that is toxic. The signaling transduction system controlling bacterial chemotaxis has been extensively studied in two model organisms, *Escherichia coli* and *Salmonella enterica* [for recent reviews, see (Wadhams and Armitage, 2004;Sourjik and Armitage,

*Corresponding author. Mailing address: Department of Oral Biology, and Department of Microbiology and Immunology, SUNY at Buffalo, 3435 Main St., Buffalo, NY 14214-3092, Electronic mail address: cli9@buffalo.edu; phone: (716)829-6014; Fax: (716)829-3942.

2010;Hazelbauer *et al.*, 2008)]. The core structural unit in the chemotaxis signaling pathway consists of a ternary complex of chemoreceptors (often referred to as methyl-accepting chemotaxis proteins, MCPs), a histidine autokinase CheA, and a coupling protein CheW (Gegner *et al.*, 1992;Liu and Parkinson, 1989). CheW is a single-domain cytoplasmic protein (Griswold and Dahlquist, 2002).

MCPs sense various environmental signals, which control the activity of CheA. Activated CheA (CheAP) transfers its phosphoryl group to CheY, a response regulator that controls the rotational direction of flagellar motors. The phosphorylated CheY (CheY-P) diffuses from the core complex to the flagellar motors, where it binds motor-switch complex proteins to promote a switch in the rotational direction from counterclockwise (CCW) to clockwise (CW). CCW rotation results in smooth swimming (also referred to as run), and CW rotation leads to tumbling. Cells responding to a positive response (binding of an attractant to MCPs) lengthen the intervals between tumbling events and hence have longer runs that allow the bacteria to swim preferentially toward higher concentrations of attractants (Sourjik and Armitage, 2010;Porter *et al.*, 2011). In the enteric bacteria, there are single homologues of *cheA*, *cheW* and *cheY,* and null mutations in any of these genes cause cells to run constantly and to become deficient in chemotaxis (Parkinson, 1977;Parkinson and Houts, 1982).

Borrelia burgdorferi, the causative agent of Lyme disease (Burgdorfer *et al.*, 1982), is highly motile and shows chemotactic responses to several attractants produced by the hosts (Charon and Goldstein, 2002; Bakker *et al.*, 2007;Shih *et al.*, 2002). Our recent study shows that chemotaxis is involved in the pathogenicity of *B. burgdorferi* (Sze *et al.*, 2012). Chemotaxis in *B. burgdorferi* differs from that of *E. coli* and *S. enterica* in several important respects [for recent reviews, see (Charon and Goldstein, 2002; Charon *et al.*, 2012)]. *B. burgdorferi* cells are relatively long (10 to 20 μm in length) and thin (0.3 μm in diameter), and two flat ribbons of periplasmic flagella (PFs) arise in the subpolar region at each cell end (Charon *et al.*, 2009;Liu *et al.*, 2009). Motility is powered by the coordinated rotation of the PFs. This architecture requires that the swimming behavior of spirochetes is very different from that of the peritrichously flagellated enteric bacteria (Dombrowski *et al.*, 2009;Yang *et al.*, 2011;Harman *et al.*, 2012;Goldstein *et al.*, 1994;Li *et al.*, 2002;Motaleb *et al.*, 2011b;Motaleb *et al.*, 2005). *B. burgdorferi* has three swimming modes: run, flex, and reversal. A run occurs when the bundle of PFs at the anterior end rotates CCW and that at the posterior end rotates CW. A reversal happens when both bundles change their rotational direction nearly simultaneously. A flex represents a non-translational mode when the two bundles of PFs rotate in the same direction (both CCW or both CW).

During a chemotaxis response, the spirochetes must coordinate the rotation of the motors at the two ends of cells (i.e., repressing the time spent in flexing and reversing, and increasing the time spent in running). A long-standing question about the spirochete chemotaxis is how the cells achieve this coordination (Li *et al.*, 2002;Charon and Goldstein, 2002;Charon *et al.*, 2012). In the spirochetes, the motors at the two ends of the cells are located at a considerable distance from one another (at least 10 μm), and the MCPs form clusters that are in close proximity to the motors (Xu *et al.*, 2011;Briegel *et al.*, 2009;Charon *et al.*, 2009;Liu *et al.*, 2009). It would seem too slow to transmit signals from one end of the cell to the other simply by diffusion of CheY-P (Motaleb *et al.*, 2011b;Sarkar *et al.*, 2010;Porter *et al.*, 2011).

Unlike *E. coli* and *S. enterica*, *B. burgdorferi* contains more than one homologue of *cheA*, *cheW*, and *cheY*: two *cheAs* (*cheA*$_1$ and *cheA*$_2$), three *cheWs* (*cheW*$_1$, *cheW*$_2$ and *cheW*$_3$), and three *cheYs* (*cheY*$_1$, *cheY*$_2$ and *cheY*$_3$) (Fraser *et al.*, 1997;Charon and Goldstein, 2002). Many of these genes reside within two gene clusters: the *flaA* operon (*flaA*-*cheA*$_2$-*cheW*$_3$-*cheX*-*cheY*$_3$) and the *cheW*$_2$ operon (*cheW*$_2$-*bb0566*-*cheA*$_1$-*cheB*$_2$-*bb0569*-*cheY*$_2$) (Ge and Charon, 1997;Li *et al.*, 2002). We have recently identified several genes that are

essential for the chemotaxis of *B. burgdorferi*, including *cheA*$_2$, *cheY*$_3$, and *cheX* (an analogue of *cheZ* from *E. coli*). The *cheA*$_2$ and *cheY*$_3$ mutants fail to reverse and constantly run, whereas the *cheX* mutant constantly flexes. None of these mutants is able to carry out chemotaxis (Motaleb *et al.*, 2011b;Motaleb *et al.*, 2005;Li *et al.*, 2002;Bakker *et al.*, 2007;Sze *et al.*, 2012).

In contrast to the *flaA* operon, the genes studied to date in the *cheW*$_2$ operon are not required for the chemotaxis of *B. burgdorferi*, e.g., the *cheA*$_1$ and *cheY*$_2$ mutants have a chemotaxis phenotype that is similar to wild type (Li *et al.*, 2002;Motaleb *et al.*, 2011b). It has been speculated that *B. burgdorferi* may possess two chemotaxis pathways that function in different hosts during the infection cycle (Li *et al.*, 2002;Charon and Goldstein, 2002;Sze *et al.*, 2012). For example, the chemotaxis genes (*cheA*$_2$-*cheW*$_3$-*cheX*-*cheY*$_3$) in the *flaA* operon may form a pathway that executes chemotaxis in mammalian hosts, whereas the genes in the *cheW*$_2$ operon (*cheW*$_2$-*cheA*$_1$-*cheY*$_2$) may constitute a pathway that controls chemotaxis in the tick vector. In *E. coli*, CheW interacts with both MCPs and CheA and plays a pivotal role in chemotaxis and formation of the MCP-CheW-CheA ternary complexes (Gegner *et al.*, 1992;Liu and Parkinson, 1989;Vu *et al.*, 2012;Boukhvalova *et al.*, 2002b). Thus, elucidating the roles of the three CheWs of *B. burgdorferi* in chemotaxis will help us determine whether this organism has two different chemotaxis pathways.

In this report, the three *cheW* genes of *B. burgdorferi* were separately inactivated by allelic exchange mutagenesis, and their roles in chemotaxis and chemoreceptor assembly were investigated by an approach consisting of computer-based bacterial tracking analysis, swim plate and capillary assays, immunofluorescence assay (IFA), and cryo-electron tomography (cryo-ET). Furthermore, the interactions between the two CheAs and three CheWs were studied by co-immunoprecipitation (co-IP). The results support the idea that *B. burgdorferi* has two different chemosensory pathways: $CheW_1$/$CheW_3$-$CheA_2$-$CheY_3$, which form a pathway that is essential for chemotaxis under the tested *in vitro* conditions; $CheW_2$-$CheA_1$-$CheY_2$ and/or $CheY_1$, whichform another pathway that is either required for chemotaxis under other conditions or is involved in a different signaling pathway.

RESULTS

Conservation of functionally important residues in $CheW_1$, $CheW_2$, and $CheW_3$

Among the three *cheW* genes, *cheW*$_2$ (*bb0565*) is the first gene in the *cheW*$_2$ operon, *cheW*$_3$ (*bb0670*) is the third gene in the *flaA* operon, and *cheW*$_1$ (*bb0312*) is located in a gene cluster where no other putative chemotaxis or motility genes are evident (Fraser *et al.*, 1997;Charon and Goldstein, 2002;Li *et al.*, 2002). $CheW_1$ consists of 176 amino acids (aa) with a predicated molecular weight (MW) of 20 kDa. $CheW_2$ is 180 aa in length with a predicted MW of 21 kDa. $CheW_3$ contains 466 aa, and its predicted MW is 53 kDa. A Blast search showed that the N-terminus of $CheW_3$ is a conserved CheW domain (aa 26 to 165) and that its C-terminus (aa 196 to 466) contains a CheR-like domain (Figure S1) (Djordjevic and Stock, 1997;Djordjevic and Stock, 1998;Shiomi *et al.*, 2002). The *E. coli* CheA contains a CheW-like domain, P5, which mediates the interaction between CheA and CheW (Bilwes *et al.*, 1999;Park *et al.*, 2006). Sequence alignment showed that the three CheW proteins also share certain similarity to the P5 domains from the CheA proteins of *E. coli* and *B. burgdorferi* (Figure S2).

The function of CheW has been extensively studied in *E. coli*, and the key residues involved in the CheW/MCP and CheW/CheA interactions have been identified (Boukhvalova *et al.*, 2002a; Boukhvalova *et al.*, 2002b;Liu and Parkinson, 1989;Liu and Parkinson, 1991;Cardozo *et al.*, 2010;Vu *et al.*, 2012). *B. burgdorferi* CheWs share 28% ($CheW_1$), 28% ($CheW_2$), and 30% (the CheW domain in $CheW_3$) sequence identity with *E. coli* CheW

($CheW_{Ec}$). Sequence alignment disclosed that the majority of the residues essential for the function of $CheW_{Ec}$ are conserved among the three CheWs (Figure 1), including I33, E38, G57, R62, G63, G99, V108, and G133. A few residue variations were also observed (e.g., V36/I in $CheW_1$, V88/M and V105/I in $CheW_3$; see Figure 1). These similarities suggest that all three CheWs may function like $CheW_{Ec}$.

$CheW_1$ and $CheW_3$ have more structural similarities with CheW

The structure of *T. maritima* CheW (designated as $CheW_{Tm}$) has been determined by nuclear magnetic resonance (NMR) (Griswold and Dahlquist, 2002;Park *et al.*, 2006), and $CheW_{Ec}$ and $CheW_{Tm}$ appear to share a very similar 3D structure (Li *et al.*, 2007). To reveal the structural features of $CheW_1$, $CheW_2$, and $CheW_3$, homology modeling analysis was conducted using $CheW_{Tm}$ as a structure template. Like $CheW_{Tm}$, all three CheW proteins are predicted to contain two β-sheet domains (domain 1 and domain 2), and each domain consists of a five-stranded β-barrel (Figure 2). In addition, five highly variable regions (HVR) were identified (Figure 2). Structural alignment revealed that the root-mean-square deviations (RMSD) of backbone atoms between $CheW_{Tm}$ (blue) and $CheW_1$ (yellow), $CheW_2$ (orange), or the N-terminal CheW domain of $CheW_3$ (red) were 0.566 Å, 1.617 Å, and 0.347 Å, respectively. In contrast to $CheW_1$ and $CheW_3$, $CheW_2$ had a long loop inserted near the N-terminus of β strand 6 in domain 2 (Figure 2B), within the binding interface predicted for CheA (Griswold and Dahlquist, 2002;Park *et al.*, 2006). These structural features suggest that $CheW_1$ and $CheW_3$ are more structurally similar to $CheW_{Ec}$ and $CheW_{Tm}$ than is $CheW_2$.

Immunoblot analysis of cheW mutants and their cognate complemented strains

As a coupling protein, CheW interacts with both MCPs and CheA. In *E. coli*, CheW plays a critical role in chemotaxis; a *cheW* null mutant constantly runs and is deficient in chemotaxis (Parkinson, 1977;Liu and Parkinson, 1989;Liu and Parkinson, 1991). To investigate the roles of $CheW_1$, $CheW_2$, and $CheW_3$ in chemotaxis, the genes encoding these three proteins were inactivated by allelic exchange mutagenesis (described in Materials and Methods). A PCR analysis showed that the individual *cheW* genes were targeted by the antibiotic resistant makers as expected (Figure S3).

A single clone representing each mutation (ΔW_1, ΔW_2, and ΔW_3, which represent the *cheW*$_1$, *cheW*$_2$, and *cheW*$_3$ mutants, respectively) was selected for further characterizations. Immunoblot analyses using anti-CheW antisera (designated as$\alpha CheW_1$, $\alpha CheW_2$, and $\alpha CheW_3$) showed that $CheW_1$, $CheW_2$, and $CheW_3$ were all detected in the wild-type strain B31A but not in the corresponding mutant clones (Figure 3). Among these three mutants, as ΔW_1 and ΔW_3 had altered chemosensory behaviors, these two mutants were complemented using the vectors $CheW_1$/pBSV2G and $CheW_3$/pBSV2G, which were constructed as described in the Materials and Methods. Immunoblot analyses showed that the complementation of *cheW*$_1$ (ΔW_1^+) and *cheW*$_3$ (ΔW_3^+) by the corresponding wild-type genes restored the synthesis of $CheW_1$ (Figure 3A) and CheW3 (Figure 3C).

The $cheW_1$ and $cheW_3$ mutants are defective in chemotaxis

Chemotaxis in the ΔW_1, ΔW_2, and ΔW_3 mutants was characterized using swim plate and capillary assays. In the swim plate assay, the ΔW_2 mutant formed similar-sized colonies as the B31A strain (Figure 4B). However, the ΔW_1 and ΔW_3 mutants formed considerably smaller rings that were similar to that of a $\Delta flaB$ strain (Figure 4A & C), a previously documented non-motile mutant (Motaleb *et al.*, 2000). Thus, *cheW*$_1$ and *cheW*$_3$, but not *cheW*$_2$, are critical for chemotaxis under the tested conditions. Consistent with the results of swim plate assay, the capillary assay demonstrated that ΔW_1 and ΔW_3 do not respond to GlcNAc as an attractant (Figure 4D & F), whereas the ΔW_2 mutantshowed the same

response to GlcNAc as the wild-type strain (Figure 4E). The cognate complemented strains, ΔW_1^+ and ΔW_3^+, exhibited spreading on the swim plates and chemotactic responses to GlcNAc at wild-type levels (Figure 4A, C, D, and F). Collectively, these results indicate that *cheW*$_1$ and *cheW*$_3$ are required for *B. burgdorferi* chemotaxis, whereas *cheW*$_2$ is dispensable for chemotaxis.

The cheW$_1$ and cheW$_3$ mutants show an altered swimming behavior

Non-chemotactic mutants often show altered swimming behaviors, e.g., the *cheA*$_2$ and *cheY*$_3$ mutants of *B. burgdorferi* fail to reverse and constantly run (Motaleb *et al.*, 2011b;Li *et al.*, 2002). The tracking analysis using a computer-assisted cell tracker coupled with video microscopy disclosed that the ΔW_2 mutant had swimming behavior indistinguishable from (Video 2, Table 1) the wild type (Video 1), whereas the ΔW_1 and ΔW_3 mutants had altered swimming behaviors. The ΔW_3 mutant failed to reverse and constantly ran in one direction (Video 3, Table 1), like the *cheA*$_2$ and *cheY*$_3$ mutants of *B. burgdorferi*. The behavior of the ΔW_1 mutant is mixed (Video 4): approximately half of the cells (21 out of 50) failed to reverse and swam exclusively in one direction. The remainder of the cells (29 out of 50) reversed, but at a lower reversal frequency (9 reversals/min) compared to the wild type (23 reversals/min). A similar pattern was observed in a reconstructed ΔW_1 mutant, suggesting that the observed mixed phenotype is stochastic and not caused by genetic heterogeneity. The complemented mutants ($\Delta W_3^+$and ΔW_1^+) had a similar swimming behavior as the wild type (Video 3A, Video 4A, and Table 1). All three *cheW* mutants had similar swimming velocities as the wild type (Table 1), ranging from 9 to12 μm/sec. Thus, none of the *cheW* mutations causes a decrease in the propulsive force generated by the flagella.

The CheR-like domain in CheW$_3$ is not required for chemotaxis

CheW$_3$ possesses a CheR-like domain at its C-terminus (Figure S1). In *E. coli*, CheR functions as a methyltransferase that is involved in chemoreceptor adaptation (Djordjevic and Stock, 1997;Djordjevic and Stock, 1998;Porter *et al.*, 2011). Searching large sets of CheW homologues from microbial genome databases revealed that only CheWs from some spirochete species have a similar domain composition as CheW$_3$, including CheW$_1$ (TP_0364) of *Treponema pallidum* and CheW$_1$ (TDE_1492)of *Treponema denticola* (Fraser *et al.*, 1998;Seshadri *et al.*, 2004). To determine whether the CheR-like domain is required for normal chemotaxis, the ΔW_3 mutantwas complemented with a plasmid producing only the N-terminal CheW domain of CheW$_3$ (aa 1–210). Immunoblotting using αCheW$_3$ showed that the expression of the N-terminal CheW domain was restored in the complemented clone (ΔW_3^{N+}) (Figure 3C). The swim plate (Figure 4C), capillary (Figure 4F), and tracking (Table 1) assays demonstrated that chemotaxis in the ΔW_3^{N+} strain was indistinguishable from that of the wild-type and ΔW_3^+ strains, indicating that deletion of the CheR-like domain does not affect the chemotactic function of CheW$_3$ under the conditions tested.

Loss of CheW$_1$ or CheW$_3$ affects chemoreceptor assembly at the cell poles

In *E. coli*, CheW is essential for the assembly of chemoreceptor arrays at the cell poles (Studdert and Parkinson, 2005;Maddock and Shapiro, 1993;Sourjik and Berg, 2000). Our previous studies showed that *B. burgdorferi* MCPs also form arrays at the cell poles (Xu *et al.*, 2011). To determine whether the *B. burgdorferi cheW* mutants are defective in chemoreceptor assembly, the cellular location of the MCPs in the three mutants was determined by IFA using an antibody targeted specifically against *B. burgdorferi* MCP$_3$ (Xu *et al.*, 2011). As expected, bright fluorescent loci were observed at both cell poles in wild-type cells (Figure 5A). A similar pattern was observed in ΔW_2 cells (Figure 5C), but not in ΔW_3 cells, in which the fluorescence was diffused (Figure 5D). Although fluorescent loci were still evident at the poles of ΔW_1 mutant cells, the fluorescence signals were

considerably reduced, and even absent in many cells (Figure 5B). The IFA results suggest that $CheW_1$ and $CheW_3$, but not $CheW_2$, are involved in the assembly and localization of the chemoreceptor arrays.

Cryo-ET was conducted to determine the cellular locations and ultrastructures of the chemoreceptor arrays in the three *cheW* mutants more precisely. Chemoreceptor arrays could be readily recognized as prominent 'basal plate'-like structures (Zhang *et al.*, 2004;Briegel *et al.*, 2009;Briegel *et al.*, 2012;Xu *et al.*, 2011;Liu *et al.*, 2012) at the poles of wild-type (Figure 6A) and ΔW_2 cells (Figure 6B). The arrays had an average length of 159 ± 86 nm (n=19 cells, Table 2). No chemoreceptor arrays were observed in any of the ΔW_3 cells examined (0 out of 25 cells, Figure 6C). However, the arrays could be readily detected in its complemented strain ΔW_3^+ (12 out of 30 cells, Figure 6D). With the ΔW_1 mutant, the arrays were still evident in a small portion of the cells (4 out 31 cells, Figure 6E), but their sizes were substantially reduced (average length of 75 ± 7 nm, n=4 cells) compared to those of the wild type or the complemented ΔW_1^+strain (Figure 6F, 152 ± 58 nm, n = 10 cells). The cryo-ET results are consistent with the IFA data and thus further confirm that both $CheW_1$ and $CheW_3$ are involvedin assembly of the chemoreceptor arrays, whereas $CheW_2$ is not.

$CheW_1$ and $CheW_3$ interact with $CheA_2$, whereas $CheW_2$ binds $CheA_1$

In *E. coli*, the ternary complex of MCP-CheW-CheA is the core structural unit in the signaling pathway of chemotaxis (Wadhams and Armitage, 2004;Hazelbauer *et al.*, 2008). *B. burgdorferi* has two CheA homologues, $CheA_1$ and $CheA_2$. Identifying the interactions between the two CheAs and the three CheWs will help us understand the complexity of chemotaxis signaling pathways in *B. burgdorferi*. Co-IP experiments were carried out to reveal the interactions between the two CheAs and the three CheWs. For the co-IP assays, either $CheA_1$ antibody ($\alpha CheA_1$) or $CheA_2$ antibody ($\alpha CheA_2$) was first co-incubated with whole cell lysates of the B31A wild type and a previously constructed double $cheA_1cheA_2$ mutant (designated as ΔA_1A_2 and used as a negative control) (Li *et al.*, 2002). The co-precipitated products were then probed with $\alpha CheW_1$, $\alpha CheW_2$, or $\alpha CheW_3$, respectively. As shown in Figure 7, $CheW_1$ (Figure 7A) and $CheW_3$ (Figure 7C) were detected in the samples precipitated by $\alpha CheA_2$ (left panel, Figure 7) but not by $\alpha CheA_1$ (right panel, Figure 7), whereas $CheW_2$ was detected in the samples precipitated by $\alpha CheA_1$ (right panel, Figure 7B) but not by $\alpha CheA_2$ (left panel, Figure 7B), suggesting that both $CheW_1$ and $CheW_3$ interact with $CheA_2$, whereas $CheW_2$ binds $CheA_1$. To confirm that $CheW_1$ and $CheW_3$ interact with $CheA_2$, $\alpha CheW_1$ and $\alpha CheW_3$ were used in the co-IP assays, and the co-IP samples were probed with $\alpha CheA_2$. As expected, $CheA_2$ was detected in the co-precipitated products from the wild type but not from the ΔW_1 and ΔW_3 mutants (Figure 7D). Collectively, the results of the co-IP assays show that $CheW_1$ and $CheW_3$ interact with $CheA_2$ but not with $CheA_1$, whereas $CheW_2$ interacts with $CheA_1$ but not with $CheA_2$.

DISCUSSION

As a coupling protein, $CheW_{Ec}$ has four known activities: binding to CheA, binding to MCPs, promoting formation of MCP-CheW-CheA ternary complexes and chemoreceptor arrays, and enabling MCPs to modulate CheA autokinase activity (Gegner *et al.*, 1992;Cardozo *et al.*, 2010;Liu and Parkinson, 1989). In this report, a comprehensive approach has been applied to investigate the roles of the products of the three *cheW* genes in *B. burgdorferi*. The results indicate that $CheW_1$ and $CheW_3$ play a similar role as the CheW of *E. coli*, because the ΔW_1 and ΔW_3 mutants showed an altered swimming behavior (Table 1 and Videos 3 & 4) and failed to respond to attractant stimuli (Figure 4D & F). Also, the IFA and cryo-ET studies showed that these two mutants are unable to assemble intact chemoreceptor arrays at the cell poles of *B. burgdorferi* (Figures 5 & 6). In contrast to ΔW_1

and ΔW_3, the ΔW_2 mutant behaved like the wild type with respect to chemotactic response to attractants (Figure 4E), swimming behavior (Table 1), and chemoreceptor assembly (Figure 5C & Figure 6B). Collectively, these results indicate that $CheW_1$ and $CheW_3$ are essential for the chemotaxis of *B. burgdorferi*, whereas $CheW_2$ is dispensable for the chemotaxis under the tested *in vitro* conditions. Consistent with this proposition, the homology modeling analysis predicts that $CheW_2$ shares the least structural similarity to $CheW_{Ec}$ and $CheW_{Tm}$ (Figure 2). It is noteworthy to point out that $CheW_2$ has a long loop insertion near the binding interface of CheW and CheA (Figure 2B). This insertion may disrupt the local environment of the CheA binding surface and consequently prevent $CheW_2$ from interacting effectively with $CheA_2$, a histidine kinase that is essential for chemotaxis of *B. burgdorferi* (Li *et al.*, 2002;Sze *et al.*, 2012).

IFA and cryo-ET assays demonstrate that $CheW_3$ plays a more important role than $CheW_1$ in the assembly of chemoreceptor arrays at the cell poles of *B. burgdorferi*. The IFA results showed that the polar-localized chemoreceptor arrays were completely disrupted in ΔW_3 cells(Figure 5D & Figure S5), nor did cryo-ET analyses find any array-like structures in the mutant (Figure 6C, Table 2). The observed phenotype of the ΔW_3 mutant is very similar to that of an *E. coli cheW* mutant (Zhang *et al.*, 2004; Sourjik and Berg, 2000;Maddock and Shapiro, 1993). Unlike the situation in ΔW_3, IFA still detected weak polar localized signals in ΔW_1 cells (Figure 5B), and arrays could still be observed by cryo-ET in a small portion of the ΔW_1 cells (Figure 6E). The average length of the chemoreceptor arrays observed in the ΔW_1 cells was approximately two fold less than those in the wild type and its complemented strain, ΔW_1^+ (Table 2). Recent cryo-ET studies of *E. coli* MCPs show that the basal plates of the arrays consist primarily of CheA and CheW (Briegel *et al.*, 2009;Briegel *et al.*, 2012;Liu *et al.*, 2012). Thus, it is conceivable that $CheW_1$ contributes to the stability of the basal plates but is not essential for their formation. Approximately one half of the ΔW_1 cells swim smoothly, and the other half still reverse but with a lower frequency than wild type (Video 4 and Table 1). The observed heterogeneous phenotype of the ΔW_1 mutant is not due to genetic heterogeneity because when the mutation was recloned, the same mixed phenotype of the original ΔW_1 mutant was observed. Moreover, genetic complementation totally restored the wild-type phenotype (Video 4A and Table 1).

In *E. coli*, CheW tethers CheA to the MCPs and affects the activity of CheA, which in turn controls the level of CheY-P. The inactivation of *cheW* completely blocks production of CheY-P. Thus, the flagellar motors are locked in CCW rotation, and a *cheW* mutant constantly runs (Gegner *et al.*, 1992;Wadhams and Armitage, 2004;Hazelbauer *et al.*, 2008). Our previous studies show that, of the two CheAs and three CheYs of *B. burgdorferi*, only $CheA_2$ and $CheY_3$ are involved in chemotaxis (Li *et al.*, 2002; Motaleb *et al.*, 2011b). The $cheA_2$ and $cheY_3$ mutants are smooth swimming and non-chemotactic, suggesting that $CheY_3$-P directly controls the rotation of flagellar motors. Because the chemoreceptor arrays in the ΔW_1 cells are only partially disrupted (Figure 5B and Figure 6E), it is possible that $CheW_1$ plays an auxiliary role in coupling $CheA_2$ to the MCPs.The decrease in $CheY_3$-P associated with the reduced coupling of $CheA_2$ results in a baseline concentration that spans the threshold required to elicit reversals.

The results presented here raise the possibility that *B. burgdorferi* may have two different chemosensory pathways (Li *et al.*, 2002;Motaleb *et al.*, 2011b;Charon and Goldstein, 2002). Among the multiple homologues of *cheA*, *cheW*, and *cheY*, only $cheA_2$, $cheY_3$, $cheW_1$, and $cheW_3$ are essential for chemotaxis *in vitro*. Other than $cheW_1$, all of the essential *che* genes are located within the *flaA* operon ($cheA_2$, $cheW_3$, *cheX*, and $cheY_3$), whereas most of the *che* genes that are dispensable for chemotaxis reside within anoperon that contains $cheA_1$, $cheY_2$, and $cheW_2$ (Charon and Goldstein, 2002;Ge and Charon, 1997;Li *et al.*, 2002;Fraser *et al.*, 1997). Co-IP assays demonstrated that $CheW_1$ and $CheW_3$ interact with $CheA_2$,

whereas $CheW_2$ binds $CheA_1$. Thus, we favor the idea that *B. burgdorferi* has two chemosensory pathways: $CheW_1/CheW_3$-$CheA_2$-$CheY_3$ form the pathway that is essential for chemotaxis under the conditions usually used *in vitro*, and $CheW_2$-$CheA_1$-$CheY_2$ and/or $CheY_1$ form another pathway that may be used only under other conditions that have yet to be duplicated in the laboratory.

Why might *B. burgdorferi* have two chemosensory pathways? In nature, *B. burgdorferi* is maintained via an enzootic cycle comprising both mammalian hosts and an *Ixodes* tick vector [for recent reviews, see (Radolf *et al.*, 2012;Samuels, 2011;Rosa *et al.*, 2005;Steere *et al.*, 2004)]. The enzootic cycle begins with the feeding by an uninfected tick on an infected vertebrate. After the feeding, the spirochetes remain in the tick gut throughout the molting process. At the time that the infected tick takes a blood meal on a mammal, the spirochetes begin to multiply and migrate from the tick gut to the salivary glands, from which they are transmitted to a new host, thereby completing the enzootic cycle. To adapt to different hosts and complete its enzootic cycle, *B. burgdorferi* may need one chemosensory pathway, perhaps represented by $CheW_1/CheW_3$-$CheA_2$-$CheY_3$, for chemotaxis in mammalian hosts. The pathway involving $CheW_2$-$CheA_1$-$CheY_2$ and/or $CheY_1$ may be activated in the tick vector and/or during the transmission from tick to mammal. Our recent study of the role of *cheA*$_2$ in the enzootic cycle of *B. burgdorferi* (Sze *et al.*, 2012) is consistent with the proposal that the $CheW_1/CheW_3$-$CheA_2$-$CheY_3$ pathway is important in the mammalian host. Inactivation of *cheA*$_2$ decreased the ability of *B. burgdorferi* to establish infection in mice, but not in ticks. The true function of the $CheW_2$-$CheA_1$-$CheY_2$ and/or $CheY_1$ pathway remains obscure. It could be involved in chemotaxis in the tick vector, perhaps in migration of the spirochetes to the salivary glands, or it may function in a signal transduction pathway that regulates gene expression of *B. burgdorferi*.

The incorporation of two coupling proteins ($CheW_1$ and $CheW_3$) into one chemosensory pathway is different from the situation in other bacteria that have more than one homologue of CheW, such as *Vibrio cholera* and *Rhodobacter sphaeroides* [for recent review, see (Porter *et al.*, 2011;Butler and Camilli, 2005;Alexander *et al.*, 2010;Rao *et al.*, 2008)]. In these organisms, either only one CheW homologue functions as a key coupling protein essential for chemotaxis, or CheW homologues are functionally redundant. For instance, *V. cholera* has three CheW homologues, but only CheW-1 is required for chemotaxis (Butler *et al.*, 2006). Among the four CheW homologues of *R. sphaeroides*, $CheW_2$ is essential for chemotaxis and chemoreceptor clustering; and deletions of other three *cheWs* either have no impact on chemotaxis or only conditionally affect chemotactic responses and chemoreceptor localization (Martin *et al.*, 2001;Hamblin *et al.*, 1997a;Hamblin *et al.*, 1997b). It is intriguing to think that the requirement for two CheW proteins in *B. burgdorferi* may have to do with the extra task of coordinating flagellar reversals at the two ends of an elongated cell body.

EXPERIMENTAL PROCEDURES

Bacterial strains and growth conditions

High-passage, avirulent *Borrelia burgdorferi sensu stricto* strain B31A (wild type) (Bono *et al.*, 2000) and its derivative mutants were grown in BSK-II liquid medium or on semi-solid agar plates at 34°Cin a humidified incubator in the presence of 3.4% CO_2, as previously documented (Li *et al.*, 2002). The *E. coli* strains were grown in LB medium at 37°C with appropriate antibiotics.

Construction of cheW mutants

The *cheW*$_1$, *cheW*$_2$ and *cheW*$_3$ genes were inactivated by allelic exchange mutagenesis as illustrated in Figure S6. To construct the vector for inactivation of *cheW*$_1$ (gene locus

bb0312; gene length, 531 bp), a 120 bp HindIII fragment was deleted and replaced by a kanamycin-resistance cassette (*aphI*) (Elias *et al.*, 2003). To construct the vector for inactivation of *cheW*$_2$ (*bb0565*; gene length, 543 bp), the *aphI* cassette was directly inserted into an EcoRV restriction cut site within the gene. To construct the vector for inactivation of *cheW*$_3$ (*bb0670*; gene length, 1,401 bp), the entire open reading frame (*orf*) was deleted and replaced with a promoterless streptomycin resistance marker (*aadA1*), as recently described (Frank *et al.*, 2003;Motaleb *et al.*, 2011a). The resultant constructs were designated as *W*$_1$*::aphI*, *W*$_2$*::aphI*, and *W*$_3$*::aadA1* (Figure S6), respectively. The PCR primers for constructing these vectors are listed in Table S1. To knock out the *cheW* genes, these vectors were first linearized and then separately transformed into B31A competent cells via electroporation as previously reported (Samuels, 1995). Transformants were selected on BSK-II agar plates containing 350 μg/ml kanamycin (for *W*$_1$*::aphI* and *W*$_2$*::aphI*) or 50 μg/ml streptomycin (for *W*$_3$*::aadA1*).

Constructing genetic complementation vectors

To construct the vector for the complementation of the *cheW*$_3$ mutant, the entire *cheW*$_3$ gene and its native promoter (P_{ami}) (Yang and Li, 2009) were first amplified by PCR with two pairs of primers (P_{17}/P_{18} for P_{ami}; P_{19}/P_{20} for *cheW*$_3$). The resultant PCR products were then fused together via PCR using primers P_{17}/P_{20}. The resultant P_{ami}*cheW*$_3$ fragment was first cloned into the pGEM®-T Easy vector (Promega, Madison, WI) and then subcloned into pBSV2G, a shuttle vector of *B. burgdorferi* that contains a gentamicin-resistance cassette (*aacC1*) (Elias *et al.*, 2003;Rosa *et al.*, 2005). The final construct was named CheW$_3$/pBSV2G (Figure S6). A similar strategy was used to construct a vector for complementation of the *cheW*$_1$ mutant (CheW$_1$/pBSV2G) and the vector for complementation of the *cheW*$_3$ mutant (CheW$_3^{N+}$/pBSV2G) with the N-terminal domain of CheW$_3$ (1–210 amino acids). The PCR primers for constructing the complementation vectors are listed in Table S1.

Generation of polyclonal antisera against CheW$_1$, CheW$_2$ or CheW$_3$

The entire *orfs* (without the translation initiation ATG/GTG codon) of *cheW*$_1$, *cheW*$_2$ and *cheW*$_3$ were amplified by PCR (the primers are listed in Table S1). The obtained PCR products were first cloned into the pGEM®-T Easy vector (Promega), and then subcloned into the pQE30 expression vector (Qiagen, Valencia, CA), which encodes an amino-terminal histidine tag. The expression of these three genes was induced using 1 mM isopropyl-β-D-thiogalactoside (IPTG). The recombinant proteins were purified by a nickel agarose column and concentrated in 10 kDa molecular weight cut off Amicon Ultra centrifugal concentrators (Millipore, Billerica, MA). Rats (for rCheW$_1$ and rCheW$_2$) and rabbits (for rCheW$_3$) were immunized with 1 to 5 mg of purified recombinant proteins during a one-month period using standard methods. The obtained polyclonal antisera were further purified using affinity chromatography with the AminoLink Plus Immobilization Kit (Thermo Scientific, Rockford, IL) and eluted as recommended by the manufacturer.

Bacterial motion tracking analysis, swim plate, and capillary assays

The swimming velocity of *B. burgdorferi* cells was measured using a computer-based motion tracking system. Swim plate assays were carried out using 0.35% agarose with BSK-IImedium diluted 1:10 with Dulbecco's phosphate-buffered saline (DPBS, pH 7.5) without divalent cations, as previously documented (Motaleb *et al.*, 2000;Li *et al.*, 2002). The plates were incubated for 3–4 days at 34°C in the presence of 3.4% CO_2. Diameters of the swim rings that appeared on the plates were measured and recorded in millimeters (mm). A previously constructed non-motile *flaB*$^-$ mutant (Δ*flaB*) (Motaleb *et al.*, 2000) was used as a negative control to determine the initial inoculum size. Capillary assays were carried out as previously documented with minor modifications (Li *et al.*, 2002;Bakker *et al.*, 2007).

Briefly, *B. burgdorferi* cells were grown to late-logarithmic-phase (~5–7 × 10^7 cells/ml) and harvested by low-speed centrifugations (1,800 × *g*). The harvested cells were then resuspended in the motility buffer (Bakker *et al.*, 2007). Capillary tubes filled with either the attractant (0.1 M N-acetyl-glucosamine [GlcNAc] dissolved in the motility buffer) or only motility buffer (negative control) were sealed and inserted into microcentrifuge tubes containing 200 μl of resuspended cells (7 × 10^8 cells/ml). After 2 hrs incubation at 34°C in a humidified chamber, the solutions were expelled from the capillary tubes, and the spirochete cells were enumerated using Petroff-Hausser counting chambers under a dark-field microscope. A positive chemotactic response was defined as at least twice as many cells entering the attractant-filled tubes as the buffer-filled tubes. For the swim plate, motion tracking, and capillary assays, results are expressed as means ± standard errors of the means (SEM). The significance of the difference between different strains was evaluated with an unpaired Student *t* test (*P* value < 0.01).

Electrophoresis and immunoblot analyses

Sodium-dodecyl-sulfate polyacrylamide-gel electrophoresis (SDS-PAGE) and immunoblotting using the enhanced chemiluminescent detectionsystem were carried out as described before (Li *et al.*, 2010;Sze *et al.*, 2011). *B. burgdorferi* cells were grown at 34°C and harvested at early stationary phase (approximately10^8 cells/ml). The whole cell lysates were prepared by washingcells once in PBS buffer (phosphate-buffered saline, pH 7.5) and then boiling for 5 min in Laemmlisample buffer. The same amount of cell lysates (~10–20 μg) were separated on SDS-PAGE gels and transferred to PVDF membrane (Bio-Rad Laboratories, Hercules, CA). The immunoblots were probed with specific antibodies against various proteins ($CheA_1$, $CheA_2$, $CheW_1$, $CheW_2$, and $CheW_3$) and developed using horseradish peroxidase-coupled secondary antibody with an ECL luminol assay.

Co-IP assay

The co-IP assay was carried out as previously described (Motaleb *et al.*, 2004). Briefly, 200 ml of the late-logarithmic-phase (~5–7 × 10^7 cells/ml) *B. burgdorferi* cultures were harvested by centrifugation and washed twice with PBS buffer containing 5 mM $MgCl_2$. The resultant cell pellets were resuspended in TSEA buffer (50 mM Tris-HCl, 150 mM NaCl, 5 mM EDTA, 0.05% sodium azide, pH 7.5) containing Nonidet P-40 (1%, v/v) and phenylmethylsulfonyl fluoride (50 μg/ml) and then incubated at 37°Cfor 1 hr. After the incubation, the obtained samples were centrifuged (1,600 × *g* for 30 min, 25°C). The resultant cell pellets were resuspended in the PBS buffer and French pressed followed by centrifugation (15,000 × g for 30 min, 25°C). Approximately 200 μl of the obtained supernatants were incubated with 50 μl of the polyclonal anti-CheAs ($\alpha CheA_1$ and $\alpha CheA_2$) or anti-CheWs ($\alpha CheW_1$, $\alpha CheW_2$, and $\alpha CheW_3$) for 1 hr at 25°C in the presence of 1% bovine serum albumin (BSA). After the incubation, 50 μl of protein A (Calbiochem-Behring Corporation, La Jolla, CA) was added to each sample and further incubated at 25°C for 1 hr. The immunoprecipitates and controls were centrifuged at 1,600 × *g* at 25°C and washed three times with 1 ml of TSEA buffer containing 0.05% Tween-20. The final pellets were suspended in 100 μl of electrophoresis sample buffer, boiled for 5 min, and briefly centrifuged. For the immunoblots, 10 μl of the supernatants was applied to each lane of SDS-PAGE gels as described above.

IFA and cryo-ET

IFA and cryo-ET assays were carried out to determine the cellular locations of MCPs in B31A and the three *cheW* mutants as previously described (Xu *et al.*, 2011). For the IFA, αMCP_3, a specific antibody against *B. burgdorferi* MCP_3, was used. For the cryo-ET analysis, freshly prepared *B. burgdorferi* cultures were deposited onto a glow-discharged holey carbon EM grid, blotted, and rapidly frozen in liquid ethane. The frozen-hydrated

specimens were imaged at −170°C using a Polara G2 electron microscope (FEI Company, Hillsboro, Oregon) equipped with a field emission gun and a 4K × 4K CCD camera (TVIPS; GMBH, Germany). The microscope was operated at 300 kV with a magnification of 31,000×. Low-dose single-axis tilt series were collected from each bacterium at −6 μm defocus with a cumulative dose of ~100 $e^{-}/Å^2$ distributed over 65 images with an angular increment of 2°, covering a range from −64° to +64°. The tilt series images were aligned and reconstructed using the IMOD software package (Kremer *et al.*, 1996). In total, cryo tomograms of B31A (30 cells), a *cheW*$_1$ mutant (31 cells) and its complemented strain (20 cells), a *cheW*$_2$ mutant (30 cells), a *cheW*$_3$ mutant (25 cells) and its complemented strain (30 cells) were reconstructed and visualized using IMOD (Kremer *et al.*, 1996).

Homology model construction of $CheW_1$, $CheW_2$, and $CheW_3$

The NMR structure of *T. maritima* CheW (Protein Data Bank ID: 1K0S) (Griswold and Dahlquist, 2002) was selected as a template for the homology modeling analysis of $CheW_1$, $CheW_2$, and N-terminus CheW like domain of $CheW_3$. Pairwise sequence alignment of CheW homologues was conducted using Clustal X. Automodel module in Modeller 9v7 (Sali and Blundell, 1993) was applied to obtain the final refined structures. All structures were analyzed and visualized in PyMol (The PyMol Molecular Graphic System, Version 1.5.0.3, Schrodinger, LLC). The qualities of the models were evaluated by PDBsum (Laskowski, 2001).

Supplementary Material

Refer to Web version on PubMed Central for supplementary material.

Acknowledgments

This research was supported by Public Health Service grants (AI073354 and AI078958) to C. Li, GM072004 to C. Wolgemuth; J. Liu was supported in part by grants AI087946 from the National Institute of Allergy and Infectious Diseases (NIAID) and AU-1714 from the Welch Foundation.

Reference List

Alexander RP, Lowenthal AC, Harshey RM, Ottemann KM. CheV: CheW-like coupling proteins at the core of the chemotaxis signaling network. Trends Microbiol. 2010; 18:494–503. [PubMed: 20832320]

Alexandre G, Zhulin IB. Different evolutionary constraints on chemotaxis proteins CheW and CheY revealed by heterologous expression studies and protein sequence analysis. J Bacteriol. 2003; 185:544–552. [PubMed: 12511501]

Bakker RG, Li C, Miller MR, Cunningham C, Charon NW. Identification of specific chemoattractants and genetic complementation of a *Borrelia burgdorferi* chemotaxis mutant: flow cytometry-based capillary tube chemotaxis assay. Appl Environ Microbiol. 2007; 73:1180–1188. [PubMed: 17172459]

Bilwes AM, Alex LA, Crane BR, Simon MI. Structure of CheA, a signal-transducing histidine kinase. Cell. 1999; 96:131–141. [PubMed: 9989504]

Bono JL, Elias AF, Kupko JD III, Stevenson B, Tilly K, Rosa P. Efficient targeted mutagenesis in *Borrelia burgdorferi*. J Bacteriol. 2000; 182:2445–2452. [PubMed: 10762244]

Boukhvalova M, VanBruggen R, Stewart RC. CheA kinase and chemoreceptor interaction surfaces on CheW. J Biol Chem. 2002a; 277:23596–23603. [PubMed: 11964403]

Boukhvalova MS, Dahlquist FW, Stewart RC. CheW binding interactions with CheA and Tar. Importance for chemotaxis signaling in *Escherichia coli*. J Biol Chem. 2002b; 277:22251–22259. [PubMed: 11923283]

Briegel A, Li X, Bilwes AM, Hughes KT, Jensen GJ, Crane BR. Bacterial chemoreceptor arrays are hexagonally packed trimers of receptor dimers networked by rings of kinase and coupling proteins. Proc Natl Acad Sci U S A. 2012; 109:3766–3771. [PubMed: 22355139]

Briegel A, Ortega DR, Tocheva EI, Wuichet K, Li Z, Chen S, et al. Universal architecture of bacterial chemoreceptor arrays. Proc Natl Acad Sci U S A. 2009; 106:17181–17186. [PubMed: 19805102]

Burgdorfer W, Barbour AG, Hayes SF, Benach JL, Grunwaldt E, Davis JP. Lyme disease, a tick-borne spirochetosis? Science. 1982; 216:1317–1319. [PubMed: 7043737]

Butler SM, Camilli A. Going against the grain: chemotaxis and infection in *Vibrio cholerae*. Nat Rev Microbiol. 2005; 3:611–620. [PubMed: 16012515]

Butler SM, Nelson EJ, Chowdhury N, Faruque SM, Calderwood SB, Camilli A. Cholera stool bacteria repress chemotaxis to increase infectivity. Mol Microbiol. 2006; 60:417–426. [PubMed: 16573690]

Cardozo MJ, Massazza DA, Parkinson JS, Studdert CA. Disruption of chemoreceptor signalling arrays by high levels of CheW, the receptor-kinase coupling protein. Mol Microbiol. 2010; 75:1171–1181. [PubMed: 20487303]

Charon NW, Cockburn Andrew, Li Chunhao, Liu Jun, Miller Kelly, Miller Michael R, et al. The unique paradigm of spirochete motility and chemotaxis. Annu Rev Immunol. 2012 In Press.

Charon NW, Goldstein SF. Genetics of motility and chemotaxis of a fascinating group of bacteria: the spriochetes. Annu Rev Genet. 2002; 36:47–73. [PubMed: 12429686]

Charon NW, Goldstein SF, Marko M, Hsieh C, Gebhardt LL, Motaleb MA, et al. The flat-ribbon configuration of the periplasmic flagella of *Borrelia burgdorferi* and its relationship to motility and morphology. J Bacteriol. 2009; 191:600–607. [PubMed: 19011030]

Djordjevic S, Stock AM. Crystal structure of the chemotaxis receptor methyltransferase CheR suggests a conserved structural motif for binding S-adenosylmethionine. Structure. 1997; 5:545–558. [PubMed: 9115443]

Djordjevic S, Stock AM. Chemotaxis receptor recognition by protein methyltransferase CheR. Nature Struct Biol. 1998; 5:446–450. [PubMed: 9628482]

Dombrowski C, Kan W, Motaleb MA, Charon NW, Goldstein RE, Wolgemuth CW. The elastic basis for the shape of *Borrelia burgdorferi*. Biophys J. 2009; 96:4409–4417. [PubMed: 19486665]

Elias AF, Bono JL, Kupko JJ III, Stewart PE, Krum JG, Rosa PA. New antibiotic resistance cassettes suitable for genetic studies in *Borrelia burgdorferi*. J Mol Microbiol Biotechnol. 2003; 6:29–40. [PubMed: 14593251]

Frank KL, Bundle SF, Kresge ME, Eggers CH, Samuels DS. *aadA* confers streptomycin resistance in *Borrelia burgdorferi*. J Bacteriol. 2003; 185:6723–6727. [PubMed: 14594849]

Fraser CM, Casjens S, Huang WM, Sutton GG, Clayton R, Lathigra R, et al. Genomic sequence of a Lyme disease spirochaete, *Borrelia burgdorferi*. Nature. 1997; 390:580–586. [PubMed: 9403685]

Fraser CM, Norris SJ, Weinstock CM, White O, Sutton GG, Dodson R, et al. Complete genome sequence of *Treponema pallidum*, the syphilis spirochete. Science. 1998; 281:375–388. [PubMed: 9665876]

Ge Y, Charon NW. Molecular characterization of a flagellar/chemotaxis operon in the spirochete *Borrelia burgdorferi*. FEMS Microbiol Lett. 1997; 153:425–431. [PubMed: 9271872]

Gegner JA, Graham DR, Roth AF, Dahlquist FW. Assembly of an MCP receptor, CheW, and kinase CheA complex in the bacterial chemotaxis signal transduction pathway. Cell. 1992; 70:975–982. [PubMed: 1326408]

Goldstein SF, Charon NW, Kreiling JA. *Borrelia burgdorferi* swims with a planar waveform similar to that of eukaryotic flagella. Proc Natl Acad Sci U S A. 1994; 91:3433–3437. [PubMed: 8159765]

Griswold IJ, Dahlquist FW. The dynamic behavior of CheW from *Thermotoga maritima* in solution, as determined by nuclear magnetic resonance: implications for potential protein-protein interaction sites. Biophys Chem. 2002; 101–102:359–373.

Hamblin PA, Bourne NA, Armitage JP. Characterization of the chemotaxis protein CheW from *Rhodobacter sphaeroides* and its effect on the behaviour of *Escherichia coli*. Mol Microbiol. 1997a; 24:41–51. [PubMed: 9140964]

Hamblin PA, Maguire BA, Grishanin RN, Armitage JP. Evidence for two chemosensory pathways in *Rhodobacter sphaeroides*. Mol Microbiol. 1997b; 26:1083–1096. [PubMed: 9426144]

Harman MW, Dunham-Ems SM, Caimano MJ, Belperron AA, Bockenstedt LK, Fu HC, et al. The heterogeneous motility of the Lyme disease spirochete in gelatin mimics dissemination through tissue. Proc Natl Acad Sci U S A. 2012; 109:3059–3064. [PubMed: 22315410]

Hazelbauer GL, Falke JJ, Parkinson JS. Bacterial chemoreceptors: high-performance signaling in networked arrays. Trends Biochem Sci. 2008; 33:9–19. [PubMed: 18165013]

Kremer JR, Mastronarde DN, McIntosh JR. Computer visualization of three-dimensional image data using IMOD. J Struct Biol. 1996; 116:71–76. [PubMed: 8742726]

Laskowski RA. PDBsum: summaries and analyses of PDB structures. Nucleic Acids Res. 2001; 29:221–222. [PubMed: 11125097]

Li C, Bakker RG, Motaleb MA, Sartakova ML, Cabello FC, Charon NW. Asymmetrical flagellar rotation in *Borrelia burgdorferi* nonchemotactic mutants. Proc Natl Acad Sci U S A. 2002; 99:6169–6174. [PubMed: 11983908]

Li C, Xu H, Zhang K, Liang FT. Inactivation of a putative flagellar motor switch protein FliG1 prevents *Borrelia burgdorferi* from swimming in highly viscous media and blocks its infectivity. Mol Microbiol. 2010; 75:1563–1576. [PubMed: 20180908]

Li Y, Hu Y, Fu W, Xia B, Jin C. Solution structure of the bacterial chemotaxis adaptor protein CheW from *Escherichia coli*. Biochem Biophys Res Commun. 2007; 360:863–867. [PubMed: 17631272]

Liu J, Hu B, Morado DR, Jani S, Manson MD, Margolin W. Molecular architecture of chemoreceptor arrays revealed by cryoelectron tomography of *Escherichia coli* minicells. Proc Natl Acad Sci U S A. 2012 May 3. [Epub ahead of print].

Liu J, Lin T, Botkin DJ, McCrum E, Winkler H, Norris SJ. Intact flagellar motor of *Borrelia burgdorferi* revealed by cryo-electron tomography: evidence for stator ring curvature and rotor/C-ring assembly flexion. J Bacteriol. 2009; 191:5026–5036. [PubMed: 19429612]

Liu JD, Parkinson JS. Role of CheW protein in coupling membrane receptors to the intracellular signaling system of bacterial chemotaxis. Proc Natl Acad Sci U S A. 1989; 86:8703–8707. [PubMed: 2682657]

Liu JD, Parkinson JS. Genetic evidence for interaction between the CheW and Tsr proteins during chemoreceptor signaling by *Escherichia coli*. J Bacteriol. 1991; 173:4941–4951. [PubMed: 1860813]

Maddock JR, Shapiro L. Polar location of the chemoreceptor complex in the *Escherichia coli* cell. Science. 1993; 259:1717–1723. [PubMed: 8456299]

Martin AC, Wadhams GH, Armitage JP. The roles of the multiple CheW and CheA homologues in chemotaxis and in chemoreceptor localization in *Rhodobacter sphaeroides*. Mol Microbiol. 2001; 40:1261–1272. [PubMed: 11442826]

Motaleb MA, Corum L, Bono JL, Elias AF, Rosa P, Samuels DS, Charon NW. *Borrelia burgdorferi* periplasmic flagella have both skeletal and motility functions. Proc Natl Acad Sci U S A. 2000; 97:10899–10904. [PubMed: 10995478]

Motaleb MA, Miller MR, Li C, Bakker RG, Goldstein SF, Silversmith RE, et al. CheX is a phosphorylated CheY phosphatase essential for *Borrelia burgdorferi* chemotaxis. J Bacteriol. 2005; 187:7963–7969. [PubMed: 16291669]

Motaleb MA, Pitzer JE, Sultan SZ, Liu J. A novel gene inactivation system reveals altered periplasmic flagellar orientation in a *Borrelia burgdorferi fliL* mutant. J Bacteriol. 2011a; 193:3324–3331. [PubMed: 21441522]

Motaleb MA, Sal MS, Charon NW. The decrease in FlaA observed in a *flaB* mutant of *Borrelia burgdorferi* occurs posttranscriptionally. J Bacteriol. 2004; 186:3703–3711. [PubMed: 15175283]

Motaleb MA, Sultan SZ, Miller MR, Li C, Charon NW. CheY3 of *Borrelia burgdorferi* is the key response regulator essential for chemotaxis and forms a long-lived phosphorylated intermediate. J Bacteriol. 2011b; 193:3332–3341. [PubMed: 21531807]

Park SY, Borbat PP, Gonzalez-Bonet G, Bhatnagar J, Pollard AM, Freed JH, et al. Reconstruction of the chemotaxis receptor-kinase assembly. Nat Struct Mol Biol. 2006; 13:400–407. [PubMed: 16622408]

Parkinson JS. Behavioral genetics in bacteria. Annu Rev Genet. 1977; 11:397–414. [PubMed: 339820]

Parkinson JS, Houts SE. Isolation and behavior of *Escherichia coli* deletion mutants lacking chemotaxis functions. J Bacteriol. 1982; 151:106–113. [PubMed: 7045071]

Porter SL, Wadhams GH, Armitage JP. Signal processing in complex chemotaxis pathways. Nat Rev Microbiol. 2011; 9:153–165. [PubMed: 21283116]

Radolf JD, Caimano MJ, Stevenson B, Hu LT. Of ticks, mice and men: understanding the dual-host lifestyle of Lyme disease spirochaetes. Nat Rev Microbiol. 2012; 10:87–99. [PubMed: 22230951]

Rao CV, Glekas GD, Ordal GW. The three adaptation systems of *Bacillus subtilis* chemotaxis. Trends Microbiol. 2008; 16:480–487. [PubMed: 18774298]

Rosa PA, Tilly K, Stewart PE. The burgeoning molecular genetics of the Lyme disease spirochaete. Nat Rev Microbiol. 2005; 3:129–143. [PubMed: 15685224]

Sali A, Blundell TL. Comparative protein modelling by satisfaction of spatial restraints. J Mol Biol. 1993; 234:779–815. [PubMed: 8254673]

Samuels DS. Electrotransformation of the spirochete *Borrelia burgdorferi*. Methods Mol Biol. 1995; 47:253–259. [PubMed: 7550741]

Samuels DS. Gene regulation in *Borrelia burgdorferi.* Annu Rev Microbiol. 2011; 65:479–499. [PubMed: 21801026]

Sarkar MK, Paul K, Blair D. Chemotaxis signaling protein CheY binds to the rotor protein FliN to control the direction of flagellar rotation in *Escherichia coli*. Proc Natl Acad Sci U S A. 2010; 107:9370–9375. [PubMed: 20439729]

Seshadri R, Myers GS, Tettelin H, Eisen JA, Heidelberg JF, Dodson RJ, et al. Comparison of the genome of the oral pathogen *Treponema denticola* with other spirochete genomes. Proc Natl Acad Sci U S A. 2004; 101:5646–5651. [PubMed: 15064399]

Shih CM, Chao LL, Yu CP. Chemotactic migration of the Lyme disease spirochete (*Borrelia burgdorferi*) to salivary gland extracts of vector ticks. Am J Trop Med Hyg. 2002; 66:616–621. [PubMed: 12201601]

Shiomi D, Zhulin IB, Homma M, Kawagishi I. Dual recognition of the bacterial chemoreceptor by chemotaxis-specific domains of the CheR methyltransferase. J Biol Chem. 2002; 277:42325–42333. [PubMed: 12101179]

Sourjik V, Armitage JP. Spatial organization in bacterial chemotaxis. EMBO J. 2010; 29:2724–2733. [PubMed: 20717142]

Sourjik V, Berg HC. Localization of components of the chemotaxis machinery of *Escherichia coli* using fluorescent protein fusions. Mol Microbiol. 2000; 37:740–751. [PubMed: 10972797]

Steere AC, Coburn J, Glickstein L. The emergence of Lyme disease. J Clin Invest. 2004; 113:1093–1101. [PubMed: 15085185]

Studdert CA, Parkinson JS. Insights into the organization and dynamics of bacterial chemoreceptor clusters through in vivo crosslinking studies. Proc Natl Acad Sci U S A. 2005; 102:15623–15628. [PubMed: 16230637]

Sze CW, Morado DR, Liu J, Charon NW, Xu H, Li C. Carbon storage regulator A (CsrA(Bb)) is a repressor of *Borrelia burgdorferi* flagellin protein FlaB. Mol Microbiol. 2011; 82:851–864. [PubMed: 21999436]

Sze CW, Zhang K, Kariu T, Pal U, Li C. *Borrelia burgdorferi* needs chemotaxis to establish infection in mammals and to accomplish its enzootic cycle. Infect Immun. 2012 Apr 16. [Epub ahead of print].

Vu A, Wang X, Zhou H, Dahlquist FW. The receptor-CheW binding interface in bacterial chemotaxis. J Mol Biol. 2012; 415:759–767. [PubMed: 22155081]

Wadhams GH, Armitage JP. Making sense of it all: bacterial chemotaxis. Nat Rev Mol Cell Biol. 2004; 5:1024–1037. [PubMed: 15573139]

Xu H, Raddi G, Liu J, Charon NW, Li C. Chemoreceptors and flagellar motors are subterminally located in close proximity at the two cell poles in spirochetes. J Bacteriol. 2011; 193:2652–2656. [PubMed: 21441520]

Yang J, Huber G, Wolgemuth CW. Forces and torques on rotating spirochete flagella. Phys Rev Lett. 2011; 107:268101. [PubMed: 22243185]

Yang Y, Li C. Transcription and genetic analyses of a putative N-acetylmuramyl-L-alanine amidase in *Borrelia burgdorferi*. FEMS Microbiol Lett. 2009; 290:164–173. [PubMed: 19025570]

Zhang P, Bos E, Heymann J, Gnaegi H, Kessel M, Peters PJ, Subramaniam S. Direct visualization of receptor arrays in frozen-hydrated sections and plunge-frozen specimens of *E. coli* engineered to overproduce the chemotaxis receptor Tsr. J Microsc. 2004; 216:76–83. [PubMed: 15369487]

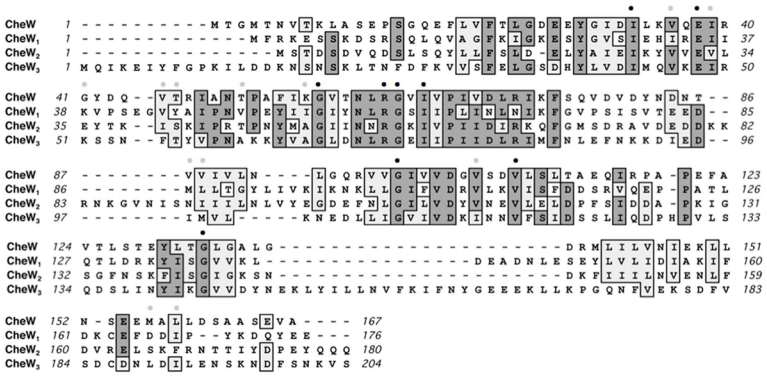

Figure 1. Sequence comparison between *E. coli* CheW and the three CheWs of *B. burgdorferi*

The numbers show the positions of residues in *E. coli* CheW and *B. burgdorferi* $CheW_1$, $CheW_2$, and the CheW domain of $CheW_3$. Dots represent functionally important residues identified in *E. coli* CheW (Liu and Parkinson, 1989;Boukhvalova *et al.*, 2002a;Boukhvalova *et al.*, 2002b;Alexandre and Zhulin, 2003). The black dots represent residues conserved in all four CheWs, and grey dots represent residues that are different in one or more of the three CheWs of *B. burgdorferi*. The boxes represent conserved residues of CheWs. The alignments were performed using the program MacVector 10.6.

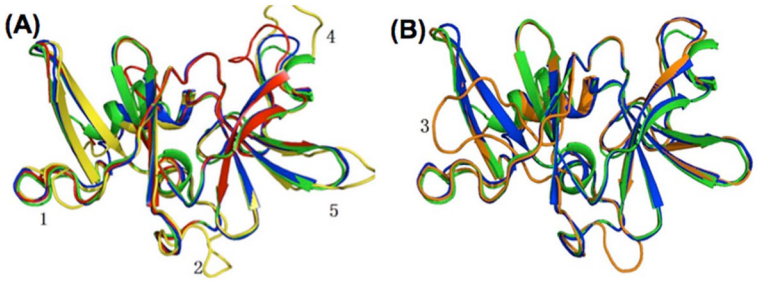

Figure 2. Homology modeling of *B. burgdorferi* CheWs

(**A**) Structure alignment of $CheW_1$ (yellow), $CheW_3$ (red), *E. coli* CheW (green), and *T. maritima* CheW (blue). (**B**) Structure alignment of $CheW_2$ (orange), *E. coli* CheW, and *T. maritima* CheW. The N-terminal regions ahead of β strand were removed for better visualization. *T. maritima* CheW (Griswold and Dahlquist, 2002)(Protein Data Bank ID: 1K0S) was selected as the basis for structural modeling using the program Modeller 9v7 (Sali and Blundell, 1993). All structures were analyzed and visualized in PyMol. The numbers represent the highly variable regions (HVR) identified.

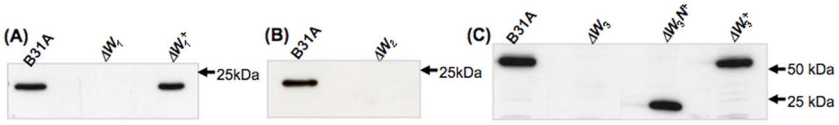

Figure 3. Immunoblot analysis of the three *cheW* mutants and their complemented strains

(A) Immunoblot analysis of the *cheW*$_1$ mutant (*ΔW*$_1$) and its complemented strain (*ΔW*$_1^+$) using αCheW$_1$. (**B**) Immunoblot analysis of the *cheW*$_2$ mutant (*ΔW*$_2$) using αCheW$_2$. (**C**) Immunoblot analysis of the *cheW*$_3$ mutant (*ΔW*$_3$), its complemented strain (*ΔW*$_3^+$), and the mutant complemented with the N-terminal CheW domain (aa 1–210) of CheW$_3$ (*ΔW*$_3^{N+}$) using αCheW$_3$. The predicted molecular weights of CheW$_1$, CheW$_2$, CheW$_3$, and the N-terminal CheW domain of CheW$_3$ are approximately 20 kDa, 21 kDa, 53 kDa, and 24 kDa, respectively.

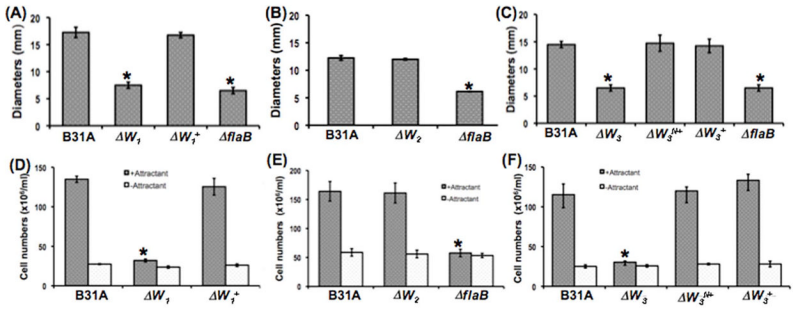

Figure 4. *B. burgdorferi cheW1* and *cheW3* mutants are non-chemotactic

Swim plate (**A**) and capillary (**D**) assays of the *cheW1* mutant (*ΔW1*) and its complemented strain (*ΔW1*$^{+}$). Swim plate (**B**) and capillary (**E**) assays of the *cheW2* mutant (*ΔW2*). Swim plate (**C**) and capillary (**F**) assays of the *cheW3* mutant (*ΔW3*) and its complemented strains (*ΔW3*$^{+}$ and *ΔW3*$^{N+}$). The swim plate and capillary assays were carried out as previously described (Motaleb *et al.*, 2000;Li *et al.*, 2002;Bakker *et al.*, 2007). For the swim-plate assay, *ΔflaB*, a previously constructed non-motile mutant (Motaleb *et al.*, 2000), was used as a control to determine the size of non-spreading colonies on the plates. For the capillary assay, N-acetyl-D-glucosamine (GlcNAc) was used as an attractant. Results are expressed as the means ± SEM from five plates or capillary tubes. * represents a *P* value < 0.01.

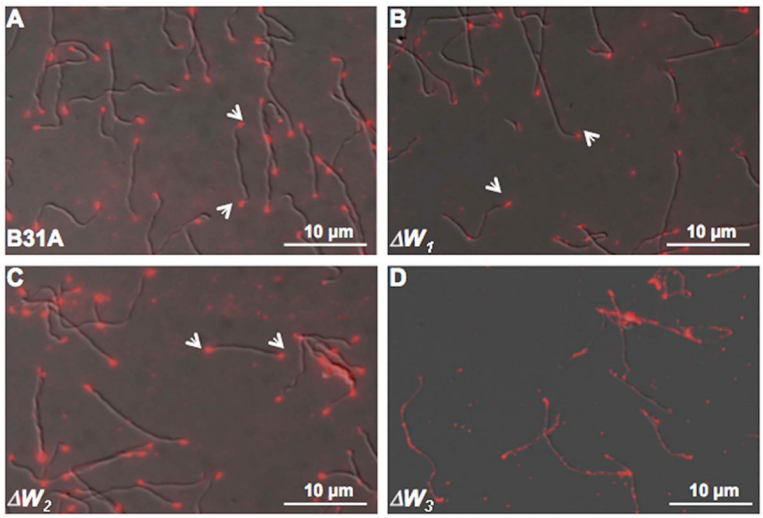

Figure 5. Localization of *B. burgdorferi* chemoreceptor arrays using IFA

The wild-type (**A**), the ΔW_1 (**B**), ΔW_2 (**C**), and ΔW_3 (**D**) mutant cells were fixed with methanol, stained with anti-MCP_3 antibody, and counterstained with anti-rat Texas red antibody as previously described (Li *et al.*, 2010;Xu *et al.*, 2011). The micrographs were taken under DIC light microcopy or fluorescence microscopy with a tetramethylrhodamine isothiocyanate (TRITC) emission filter, and the resultant images were merged. Arrows point to the location of the chemoreceptor arrays within cells.

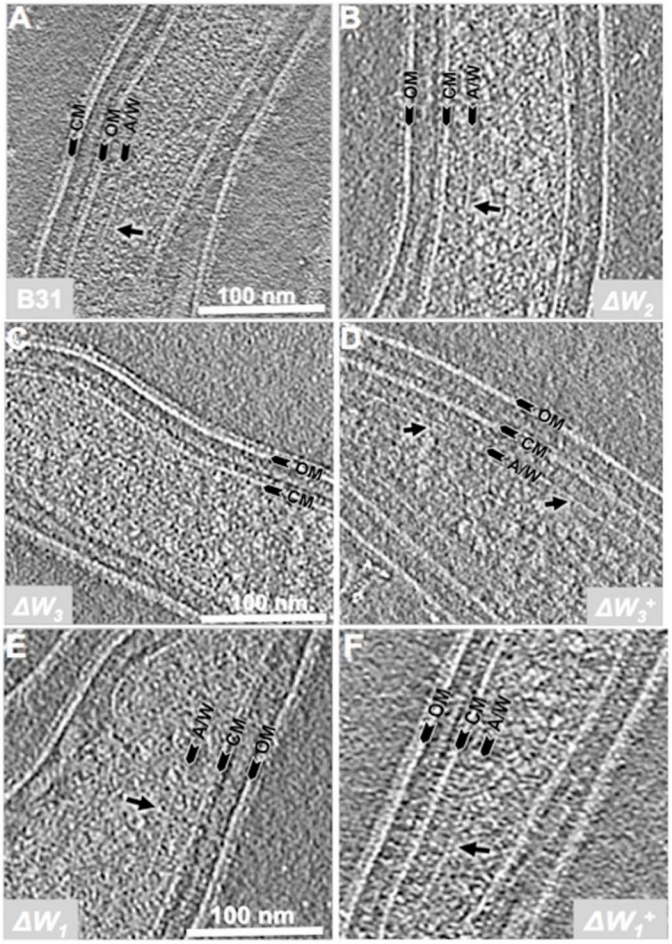

Figure 6. Detection of *B. burgdorferi* chemoreceptor arrays by cryo-ET

The cryo-ET analysis was carried out as previously described (Xu *et al.*, 2011). Six strains were included: (**A**) B31A, (**B**) ΔW_2, (**C**) & (**D**) ΔW_3 and its complemented strain ΔW_3^+, and (**E**) & (**F**) ΔW_1 and its complemented strain ΔW_1^+. Arrows point to chemoreceptor arrays. OM: outer membrane; CM: cytoplasmic membrane; A/W: the basal plate composed of CheA and CheW.

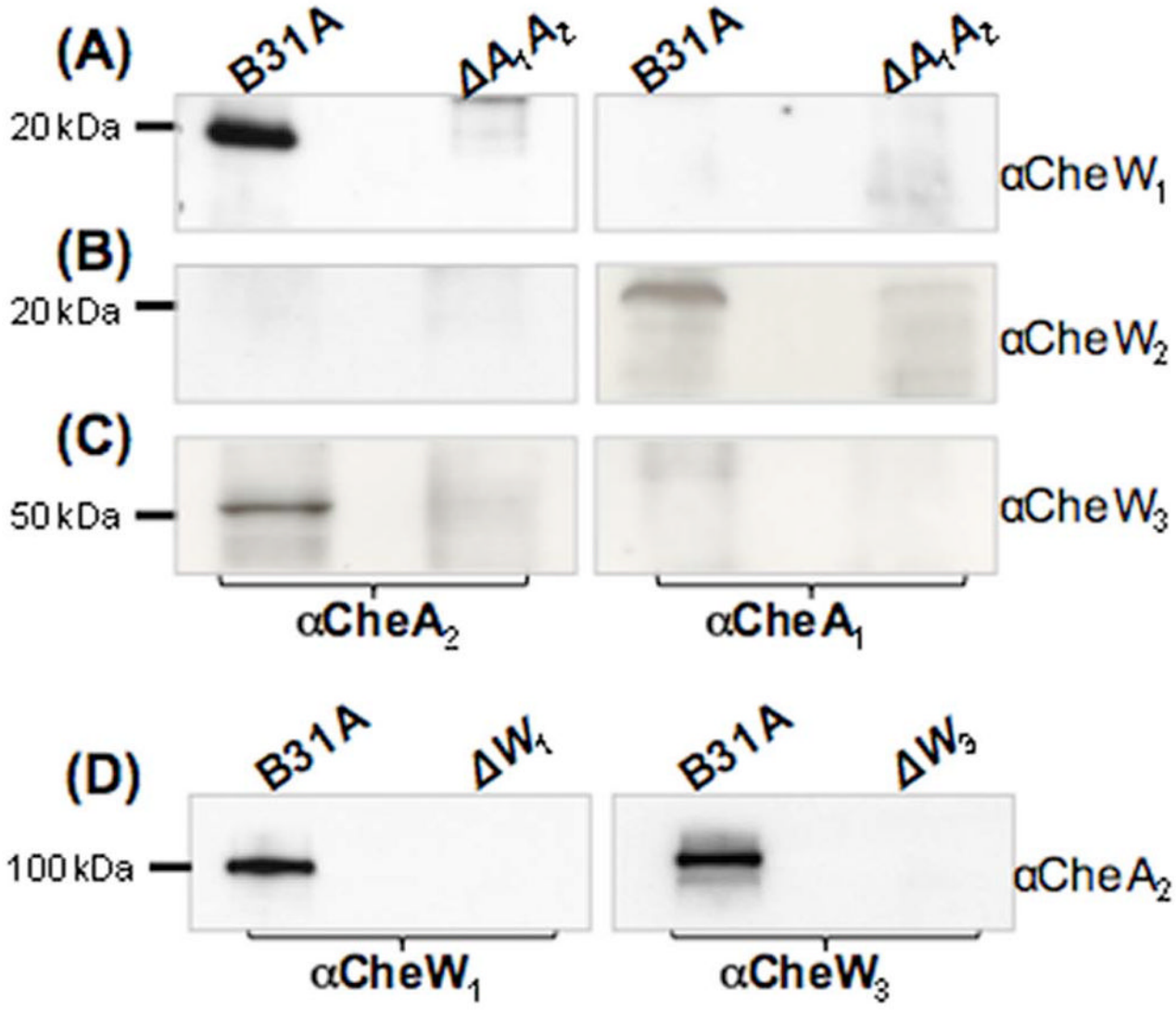

Figure 7. Detecting the interactions between two CheAs and three CheWs of *B. burgdorferi* by co-IP

Pull down of the CheWs using αCheA$_1$ (right panel) or αCheA$_2$ (left panel). Precipitated proteins were probed with αCheW$_1$ (**A**), αCheW$_2$ (**B**), or αCheW$_3$ (**C**). A previously constructed *cheA$_1$A$_2$* double-deletion mutant (*ΔA$_1$A$_2$*) of *B. burgdorferi* (Li *et al.*, 2002) was used as a negative control for the co-IP. (**D**) Pull down of CheA$_2$ using αCheW$_1$ (left panel) and αCheW$_3$ (right panel). Precipitated proteins were probed with CheA$_2$. Extracts from the *ΔW$_1$* or *ΔW$_3$* mutants were used as negative controls for the co-IP.

Table 1

Effects of CheWs on swimming behaviors of *B. burgdorferi*.

Strains	Mean velocity (μm/sec) ± SEM[a]	Mean number of reversals/min ± SEM[a]
B31	10.0 ± 0.8	23.3 ± 4.2
ΔW_1	12.3 ± 1.5	9.0 ± 6.0 [b]
ΔW_2	10.0 ± 1.4	20.0 ± 3.2
ΔW_3	11.0 ± 0.8	0.0[c]
ΔW_1^+	9.8 ± 2.2	25.0 ± 2.6
ΔW_3^+	9.7 ± 1.8	26.0 ± 1.9
ΔW_3^{N+}	9.0 ± 1.7	24.0 ± 2.1

[a] Standard errors of the means were calculated from data obtained from at least 30 individual tracked cells of each strain.

[b] Approximately one half of the cells ran in one direction and did not reverse; the other half of the cells did reverse and the mean reversal frequency was calculated from this group of the cells.

[c] Cells ran in one direction and did not reverse.

Table 2

Impact of CheWs on *B. burgdorferi* chemoreceptor assembly.

Strains	Total cells	Positive cells	Chemoreceptor array length (nm)
B31A	30	19	159 ± 86
ΔW_1	31	4	75 ± 7
ΔW_2	30	12	130 ± 30
ΔW_3	25	0	NA
ΔW_1^+	20	10	152 ± 58
ΔW_3^+	30	12	155 ± 77